Journal of Food Measurement and Characterization (2024) 18:2146–2161
https://doi.org/10.1007/s11694-023-02325-5

ORIGINAL PAPER

Fabrication of novel antimicrobial nanocomposite films based on polyvinyl alcohol, bacterial cellulose nanocrystals, and boric acid for food packaging

Milad Rouhi[1] · Farhad Garavand[2] · Mahshid Heydari[3] · Reza Mohammadi[1] · Zahra Sarlak[1] · Ilaria Cacciotti[4] · Seyed Hadi Razavi[5] · Mohammad Mousavi[5] · Ehsan Parandi[6]

Received: 18 August 2023 / Accepted: 6 December 2023 / Published online: 4 January 2024

Abstract

In this study, an environmentally friendly antimicrobial nanocomposite films were made using polyvinyl alcohol (PVOH) reinforced with glycerol, bacterial cellulose nanocrystals (BCNCs), and boric acid. Response surface methodology (RSM) and central composite design (CCD) were engaged to model and optimize the independent variables and water resistance of films. The quadratic models were significant for the water vapor permeability (WVP) and water vapor transmission rate (WVTR), while the linear models were significant for water solubility and moisture content. The findings indicated that 2.81% w/w BCNCs, 14.63% w/w boric acid, and 1.15% w/w glycerol provided the PVOH films with the best water resistance. The corresponding response values for moisture content, water solubility, WVTR and WVP predicted under the optimum condition were 10.25%, 6.23%, 210.89 g/h m^2 and 6.18 g mm/h m^2 kPa, respectively. The findings suggest that when comparing the blank glycerol and BCNCs films with the optimal film, it is evident that the addition of glycerol and BCNCs in the optimal film led to an increase and decrease in antibacterial activity against the microorganisms tested, respectively. The optimum film sample exhibited varying degrees of resistance to *Bacillus subtilis* and *Candida albicans*, with *B. subtilis* displaying the highest resistance and *C. albicans* showing relatively lower resistance. The enhanced biodegradability observed in the

✉ Seyed Hadi Razavi
srazavi@ut.ac.ir

✉ Ehsan Parandi
ehsan_parandi@ut.ac.ir

1 Department of Food Science and Technology, School of Nutrition Sciences and Food Technology, Research Center for Environmental Determinants of Health (RCEDH), Health Institute, Kermanshah University of Medical Sciences, Kermanshah, Iran

2 Department of Food Chemistry and Technology, Teagasc Moorepark Food Research Centre, Fermoy, Co. Cork, Ireland

3 Student Research Committee, Department of Food Science and Technology, School of Nutrition Sciences and Food Technology, Kermanshah University of Medical Sciences, Kermanshah, Iran

4 Department of Engineering, INSTM RU, University of Rome 'Niccolò Cusano', 00166 Rome, Italy

5 Bioprocess Engineering Laboratory (BPEL), Department of Food Science, Engineering and Technology, Faculty of Agricultural Engineering and Technology, University of Tehran, Karaj, Iran

6 Department of Food Science and Technology, Faculty of Agricultural Engineering and Technology, University of Tehran, Karaj, Iran

optimum film, compared to the neat PVOH film used as a control, can potentially be attributed to two factors: the increased moisture sensitivity of the films resulting from the addition of glycerol, and the biodegradability of glycerol itself by microorganisms. The addition of other ingredients to neat PVOH film led to a reduction in the height of the characteristic crystalline peak, thereby causing a loss in the film's stability. The findings indicated that the optimized film exhibited a higher glass transition temperature of 91 °C compared to the neat PVOH film (78 °C), BCNCs (71 °C), and boric acid (69 °C) blank films. This suggests that the incorporation of BCNCs and boric acid into the film led to an enhancement in its thermal stability. Crosslinked PVOH reinforced with BCNCs showed great potential to produce biodegradable films with modified barrier, thermal, and antibacterial properties for applications in food packaging.

Graphical abstract

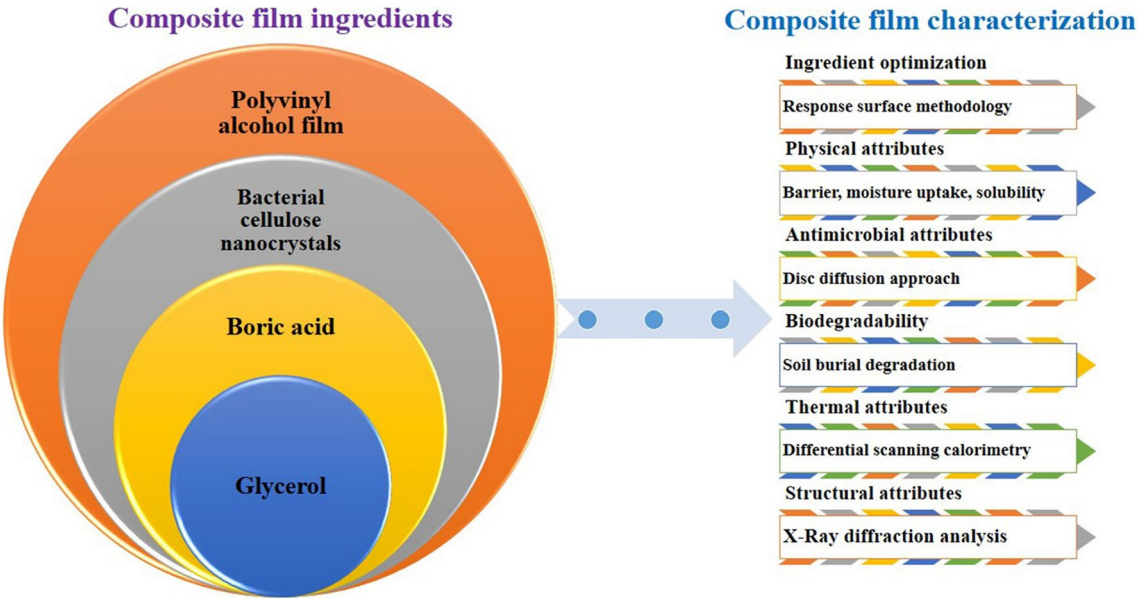

Keywords Active packaging · Biodegradable film · Nanomaterial · Cellulose · Crosslink

Introduction

An effective food packaging material should function as a robust barrier, effectively impeding the migration of environmental pollutants into food products. Extensive research has been conducted to investigate novel structural materials and antibacterial components to enhance the functional attributes of food packaging materials [1–3]. In the past few years, there has been a notable increase in research efforts aimed at addressing the environmental pollution resulting from the excessive utilization of plastics, as well as ensuring compliance with consumer safety standards. These research efforts have mostly focused on the development of diverse functionalities, including but not limited to biodegradability, antibacterial properties, and color indication. Due to this rationale, there has been a notable increase in the utilization of biodegradable packaging materials such as polylactic acid (PLA), polyvinyl alcohol (PVOH), polyhydroxy alkanoate (PHA), cellulose, chitosan, starch, and other similar substances [4, 5]. The advantages of PVOH as a hydrophilic synthetic polymer include outstanding film-producing qualities such as stretchability, thermal stability, transparency in the visible light spectrum, odorless characteristic, and oxygen barrier capabilities [6]. PVOH is also an environmentally friendly, non-toxic, and biodegradable polymer, especially in the presence of water and carbon dioxide. The significant numbers of hydroxyl (–OH) groups enable PVOH to form hydrogen bonds, which stabilize intermolecular complexes with carboxyl-containing materials [7]. PVOH has been considered in wet production due to its solubility in polar solvents such as water and alcohol with lower cost and less hazardous than non-polar solvents, causing less pollution to the environment. However, certain functional attributes, such as antibacterial or UV barrier qualities, are absent in PVOH film [8]. On the other hand, PVOH film is more sensitive to water than hydrophobic synthetic polymer films and has higher moisture diffusion [6]. To solve this deficiency, researchers have used various methods so far, such as polymer blending, and physical and chemical crosslinking [9–13].

Crosslinking is a successful method for changing the chemistry of composite materials, resulting in enhanced mechanical, thermal, and physical properties [4, 10]. Physical crosslinking methods, such as ultraviolet (UV) radiation, are commonly employed; however, they possess some limits due to the resultant weak contacts, high expenses, challenges in regulating the extent of crosslinking, and potential harm to the material [14]. As a result, the development of a simple and flexible approach is important in order to enhance the barrier and water resistance of pure PVOH film, while ensuring the preservation of its other features. One potential approach to enhancing the characteristics of PVOH involves the implementation of chemical crosslinking inside its polymer matrix [12, 14]. The –OH groups of PVOH can be crosslinked by adding chemical substances that reinforce the film matrix and form covalent or hydrogen bonds with them. These links serve as a bridge between the polymers and lessen the hydration of PVOH. The type of crosslinking agent affects the characteristics of the film. This research chose boric acid instead of other reported crosslinkers because of its relatively low toxicity inexpensive and easily soluble in cold water [12].

Higher-order plants utilize borate ions in the natural environment to strengthen their cellular structure through the process of cross-linking. Boric acid has the ability to produce borate ions when dissolved in water [15].

In addition, The enhancement of mechanical characteristics in PVOH can be achieved through the integration of nanofillers, including silica, carbon nanotubes, and nanoparticles. However, the introduction of these inorganic nanofillers might negatively impact the biocompatibility and biodegradability of PVOH. The enormous research focus lies in the utilization of nanofillers obtained from natural materials to preserve the biodegradability of PVOH [7, 16–18]. Bacterial cellulose nanocrystals (BCNCs), serving as nanofillers, are generating significant interest in the field of nanotechnology [12, 16]. Specifically, cellulose nanocrystals (CNCs) possess a considerable specific surface area, estimated to be 150 $m^2\ g^{-1}$, and exhibit a high elastic modulus of roughly 134 GPa. Importantly, these properties enable CNC to offer substantial reinforcement even at low filler percentages [16]. The degradability, sustainability, high biocompatibility, and synthesis with nonhazardous chemical treatments are considered unique properties of BCNCs [19]. The hydrophilic nature of BCNCs made them excellent candidates to be loaded into hydrophilic polymers (e.g. PVOH) as compatible nanofillers for constructing 3-dimensional networks within the composite matrix supported by robust hydrogen bonds between hydroxyl groups [20, 21]. However, the properties of crosslinked nanocomposite PVOH films can be affected by the concentration and type of plasticizers.

Plasticizers are low molecular weight compounds with the capability of increasing the free volume or molecular mobility of polymer matrices. As a consequence of plasticizer incorporation, the polymer network becomes less dense as a result of weakened intermolecular forces, leading to improved flexibility and extensibility of the composite films. The stability and hydrophilic nature of glycerol turn it into an ideal plasticizer to reinforce hydrophilic biopolymers for producing edible packaging films. Glycerol also possesses an array of advantages including high boiling point, water solubility, lack of odor, low color-changing properties, etc. [10, 21–24].

In our previous research, the influence of glycerol, BCNCs, and boric acid on the mechanical characteristics of PVOH films was investigated, and their combination was optimized to obtain maximum ultimate tensile strength (UTS), and elongation at break (EAB). Furthermore, Fourier-transform infrared (FTIR) demonstrated the interaction between ingredients [12]. However, the goals of this study were to (a) examine the impact of various components, including boric acid (crosslinking agent), BCNCs (nanofillers), and glycerol (plasticizer), on the preparation of multifunctional biodegradable water-resistant nanocomposite films based on PVOH; (b) optimize these constituents to improve the physical properties of film, and (c) investigate the antimicrobial activity, biodegradability, and thermal characteristics of the optimal sample.

Materials and methods

Materials

Extra pure glycerol (87%), and boric acid (99.8%) were obtained from Merck Group (Darmstadt, Germany). Nanocrystals with more than 99% purity and a mean crystal size of 45 nm were bought from NanoNovin Polymer (Sari, Iran). Magnesium nitrate and PVOH polymer with average molecular weight (145,000 g/mol) were obtained from Sigma-Aldrich (Prague, Czech Republic). *Staphylococcus aureus* ATCC 25923, *Pseudomonas aeruginosa* ATCC 27853, and *Escherichia coli* ATCC 25922 were obtained Pasteur Institute of Iran (Tehran, Iran).

Candida albicans ATCC10231 and *B. subtilis* ATCC 6633 were also provided by the Iranian Biological Resources Centre (Tehran, Iran).

Experimental design

Factors were found according to the former experimental studies on PVOH films based on our previous study [12]. As shown in Table 1, various concentrations of glycerol (0–50% w/w based on PVOH), boric acid (0–15% w/w), and BCNCs (0–5% w/w) were used at coded levels of + 1.68, + 1, 0, − 1, and − 1.68 to produce composite films. Briefly, 15 out of

Table 1 The experimental domain of central composite rotatable design (CCRD)

Independent variables	Unit	Symbol		Coded variable levels				
		Uncodified	Codified	− 1.68 (−α)	− 1	0	+1	+1.68 (+α)
Glycerol	g/100 g PVOH	X_1	x_1	0.00	10.13	25.00	39.87	50.00
BCNCs[a]	g/100 g PVOH	X_2	x_2	0.00	1.01	2.50	3.99	5.00
Boric acid	g/100 g PVOH	X_3	x_3	0.00	3.04	7.50	11.96	15.00

BCNCs bacterial cellulose nanocrystals

125 possible combinations of variables were selected for examination by CCRD. Furthermore, six replicas of the central point were tested to scrutinize the method's repeatability, resulting in 20 treatments in total. The experiments were performed in a randomized manner and the obtained data were examined to determine the optimal film-forming conditions.

The following equations of the generalized polynomial models are provided to estimate the response variables:

$$Y_i = \beta_{k0} + \sum_{i=1}^{3} \beta_{ki} x_i \quad (1)$$

$$Y_i = \beta_{k0} + \sum_{i=1}^{3} \beta_{ki} x_i + \sum_{i=1}^{3} \beta_{kii} x_i^2 + \sum_{i<j=2}^{3} \beta_{kij} x_i x_j, \quad (2)$$

where Y_i is the dependent variable (response), including moisture content (Y_1), water solubility (Y_2), WVTR, (Y_3), WVP (Y_4), and swelling in water (Y_5), β_{k0} represents the offset term, β_{ki} are the regression coefficients for linear effect terms, β_{kii} are quadratic effects, and β_{kij} are interaction effects, and X_i and X_j are the coded independent variables [25, 26].

Fabrication of composite films

To separate and disperse the nanocrystals, BCNCs were first sonicated (100% power, Elmasonic TIH10, Germany) at 35 kHz for 5 min at 60 °C, followed by high shear homogenization at 13,000 rpm for 7 min. The treated BCNCs and glycerol were first added to the deionized water and were mixed on a hotplate stirrer, then the PVOH powder was poured into the suspension and stirred entirely and homogenized at 80 °C, 1600 rpm for 30 min. After that, boric acid was added to the stirred suspension and similarly homogenized, until 100 ml of each suspension with 6% (w/v) was produced. The obtained suspension was again sonicated at 35 kHz for 5 min and degassed by a vacuum oven (Townson & Mercer, UK) at 500 mmHg and 60 °C for 10 min. 50 mL of the suspension was poured into polystyrene plates and stored at 50 °C for 12 h. The dried films were finally peeled off and conditioned at 25 °C and RH (relative humidity) of 53.3%.

Physical properties

Moisture content

Samples (2 × 2 cm^2) were kept in a desiccator containing saturated sodium bromide solution. Afterwards, the film specimens were weighed (W_0). Then, the films were dried and weighed again (W_1). The formula below was used to figure out moisture content [27]:

$$\text{Moisture content}(\%) = \frac{W_0 - W_1}{W_0} \times 100 \quad (3)$$

Swelling property

Samples (2 × 2 cm^2) were kept in a silica gel desiccator and weighed (W_{dry}). Then, the sample was put into a jar with 50 mL of distilled water for 4 h and then weighed (W_{wet}). The formula below was used to figure out the swelling index:

$$\text{Swelling}(\%) = \frac{W_{wet} - W_{dry}}{W_{dry}} \times 100 \quad (4)$$

Film solubility

Samples (2 × 2 cm^2) were dried at 110 °C for 5 h in a vacuum oven and weighed (W_0). Then samples were placed in a beaker with 50 mL distilled water followed by a gentle stirring at 25 °C for 4 h. The remaining undissolved films were then dried at 110 °C for 5 h until reaching a constant weight (W_f). The formula below was used to figure out water solubility:

$$\text{Water solubility}(\%) = \frac{W_0 - W_f}{W_0} \times 100 \quad (5)$$

Water vapor permeability (WVP)

Firstly, the thicknesses of samples were measured with a manual micrometre (0.01 mm accuracy, Mitutoyo Co.,

Japan) in three places of films, to provide an average value. Then, the simulation cup method was employed to determine WVP according to the ASTM E96-05. WVP was calculated as below:

$$WVP = \frac{WVTR \times L}{\Delta P}, \quad (6)$$

where water vapor transmission rate (WVTR; g mm/ kPa h m^2) through the film is computed by the slope of a straight line via the linear regression ($r^2 \geq 0.99$) divided by the exposed film area (m^2), L is the average film thickness (mm), and ΔP is the pressure difference (kPa) across both sides of the film.

Antimicrobial activity analysis

An array of microorganisms were employed to assess the antimicrobial activity of the samples. To do this, the freshly grown colonies of the *C. albicans* and bacterial strains were inoculated in Sabouraud dextrose broth and Mueller–Hinton broth, respectively, in a water bath for 4 to 6 h until reaching the McFarland turbidity of 0.5 (1.5×10^8 CFU/mL). Then, 0.1 mL of the inoculums were uniformly spread on the agar plate surface with a disposable spreader. The films were cut into 10-mm-diameter discs, set on inoculum-loaded agar plates, and put in an incubator at 37 ± 1 °C for 24 and 48 h for bacteria and for fungus, respectively [17].

Clear areas are sites where bacterial growth was inhibited. Finally, the inhibition area was calculated using the equation below:

$$\text{Inhibition area}\left(mm^2\right) = \pi \times \left(r^2 - 25\right), \quad (7)$$

where π is the constant number equal to 3.14, and r is the radius of the inhibition area.

Biodegradation test

The 10 kg container filled with soil was used to locate film samples that were already cut into 3 × 3 mm^2 pieces and dried at 80 °C, followed by being submerged in the soil at 10 cm depth. The soil was kept moist (30–50% humidity) with regular sprinkling of water. The degradation of the film was determined every 30 days for six months [28, 29]. The degradation rate in the soil burial experiment was estimated based on the weight loss during the storage according to the following equation:

$$\text{Biodegradability}(\%) = \frac{W_0 - W_t}{W_0} \times 100, \quad (8)$$

where W_0 is the weight of the dried films before burial in the soil, and W_t is the weight of the dried sample at the time of t month after burial in the soil.

Differential scanning calorimetry (DSC)

Differential scanning calorimetry (METTLER TOLEDO, Switzerland) was employed to monitor the thermal characteristics of the optimum composite films. The experiment was performed at a heating rate of 20 °C /min for the temperature range of 0–250 °C under a N_2 atmosphere (50 mL/ min).

X-ray diffraction (XRD)

The optimized film was dried and placed in the diffraction scanning chamber (Siemens X-ray D5000, Germany) to determine the X-ray patterns. The test was performed with a Cu K_α radiation beam at λ = 0.1588897 nm in the diffraction angle (2θ) range of 5–70°.

Statistical analysis

Glycerol, BCNCs, and boric acid concentrations were considered independent variables. The effects of independent variables on the film properties (moisture content, water solubility, WVP, and WVTR) and optimizing responses were studied. The RSM data were analyzed by the Design-Expert program. The antimicrobial and biodegradation tests were performed in triplicate and data were analyzed by ANOVA using SPSS software (ver.19.0) (SPSS Science, Chicago, USA).

Results and discussion

The model development

Response surface methodology was used to determine the level of variables including glycerol (X_1), BCNCs (X_2), and boric acid (X_3) concentrations, and their effects on the moisture content (Y_1), water solubility (Y_2), WVTR (Y_3), and WVP (Y_4). There is no appropriate model for swelling property response. Twenty experiments were accomplished with various combinations of the considered factors (Table 2). The assessment of various models revealed that the quadratic models ($p < 0.0001$) were significant for the WVP and WVTR, while the linear models ($p < 0.0001$) were significant for water solubility and moisture content, without significant lack of fit ($p > 0.05$). Accordingly, quadratic and linear models were selected as the most suitable models for the responses. The mathematical models for different physical attributes are expressed below:

$$Y_1 = 9.74 + 0.28X_1 \quad (9)$$

Table 2 Experimental design with the observed responses and predicted values for the moisture content, solubility, WVTR, and WVP using RSM-CCRD

Run	Independent variables			Moisture Content (Y_1, %)		Solubility (Y_2, %)		WVTR (Y_3, g/h m^2)		WVP (Y_4, g mm/h m^2 kPa)	
	X_1	X_2	X_3	Experimental*	Predicted	Experimental[b]	Predicted	Experimental[c]	Predicted	Experimental**	Predicted
1	0	0	+1.68	18.18	16.53	12.22	16.42	484.99	454.14	13.83	12.82
2	0	0	0	15.38	17.64	27.37	25.55	725.14	603.71	16.54	17.03
3	0	0	0	18.73	17.64	25.30	25.55	542.86	603.71	15.48	17.03
4	0	+1.68	0	15.58	19.73	23.18	21.88	521.12	457.65	14.86	13.96
5	0	0	0	17.59	17.64	29.56	25.55	513.11	603.71	17.56	17.03
6	−1	+1	−1	16.67	15.43	23.00	22.44	294.91	320.99	8.41	8.90
7	0	0	−1.68	18.75	18.75	35.00	34.67	642.81	618.34	18.33	17.01
8	−1	−1	−1	14.29	12.94	28.33	26.80	541.46	517.1	12.35	13.54
9	+1	+1	−1	25.77	23.66	30.00	35.14	582.84	623.31	16.62	17.68
10	−1	−1	+1	8.33	11.62	17.27	15.95	382.94	381.59	10.92	11.51
11	0	−1.68	0	14.29	15.55	29.67	29.22	475.32	483.47	18.97	17.54
12	+1.68	0	0	21.43	24.56	39.36	36.23	625.28	556.33	17.83	16.54
13	0	0	0	17.08	17.64	28.94	25.55	632.29	603.71	18.03	17.03
14	0	0	0	15.70	17.64	28.37	25.55	564.25	603.71	16.09	17.03
15	+1	−1	−1	23.67	21.17	35.00	39.51	577.70	608.38	19.77	20.59
16	−1	+1	+1	16.67	14.11	12.00	11.59	327.53	335.96	9.34	10.17
17	+1	+1	+1	24.67	22.34	24.00	24.29	500.07	563.55	14.26	14.72
18	−1.68	0	0	12.30	10.72	9.00	14.87	274.57	288.19	7.83	6.78
19	+1	−1	+1	22.67	19.85	27.27	28.65	385.10	398.14	13.18	14.34
20	0	0	0	15.04	17.64	26.09	25.55	635.10	603.71	18.11	17.03

WVTR water vapor transmission rate, *WVP* water vapor permeability, *RSM-CCRD* response surface methodology-central composite design

[a]Mean of quadruplicate determinations

[b]Mean of triplicate determinations

$$Y_2 = 27.66 + 0.43X_1 - 1.47X_2 - 1.22X_3 \quad (10)$$

$$Y_3 = 385.38 + 16.02X_1 - 0.10X_3 - 0.29X_1^2 - 21.30X_2^2 \quad (11)$$

$$Y_4 = 7.82 + 0.70X_1 - 1.11X_2 + 0.37X_3 - 0.009X_1^2 \quad (12)$$

The study of the polynomial models' variances is shown in Table 3. The results of the statistical study showed that the R^2 values (> 0.73) for the polynomial models were high for all responses which indicates that the response surface models present a high percentage of responses (Table 3). It should be noted that the addition of variables to the model can increase the R^2 values, nevertheless, the added variables are statistically significant. Hence, the higher R^2 values of models don't show the sufficiency of the model. To tackle this, adjusted R^2 values could be better indicators of the model's sufficiency. Table 3 also shows the adjusted R^2 values of moisture content, water-solubility, WVTR, and WVP (0.68, 0.84, 0.68, and 0.84, respectively). To be in an appropriate agreement, the predicted R^2 must be close to 0.2 of the adjusted R^2, which assesses how accurately the model predicts a response value. Given the mentioned explanations, all predicted values, excluding those for WVTR and WVP, agreed with the adjusted R^2 (Table 3). Furthermore, Table 3 reveals that CV values were between 9.58 and 13.86. The signal-to-noise ratio is represented by AP values, and ratios higher than 4 signify that the model discrimination is adequate. The AP values were in the range of 6.79–19.96, which is an acceptable range for model discrimination sufficiency.

Moisture content

The whole void extent of the water molecules in the film network and their hydrophilic behavior are related to the moisture content. From Table 3 and Fig. 1, the moisture content of PVOH films was significantly ($p < 0.0001$) affected linearly by the glycerol concentration, in which the higher glycerol incorporation into the PVOH films resulted in higher values of moisture content. Film moisture content values as a function of glycerol concentrations are predicted using Eq. 12. The R^2 value and the predicted R^2 were 0.72 and 0.53, respectively, which is in good agreement with the adjusted R^2 of 0.67. The AP of 12.65 is also implying a proper signal.

Table 3 ANOVA of the polynomial models for the response variables

Source	Degree of freedom		Moisture content (Y_1, %)		Solubility (Y_2, %)		WVTR (Y_3, g/h m^2)		WVP (Y_4, g mm/h m^2 kPa)	
	Linear	Quadratic	SS	p-value	SS	p value	SS	p value	SS	p value
Model	3	9	258.13	< 0.0001[a]	1017.78	< 0.0001[a]	242,746.87	0.0066[a]	224.68	0.0003[a]
Linear										
β_1	1	1	231.02	< 0.0001[a]	550.82	< 0.0001[a]	86,790.26	0.0018[a]	114.95	< 0.0001[a]
β_2	1	1	21.16	0.0782	64.96	0.0203[a]	804.66	0.6930	15.41	0.0205[a]
β_3	1	1	5.94	0.3336	402.01	< 0.0001[b]	32,546.01	0.0272[a]	21.21	0.0091[a]
Quadratic										
β_{11}		1					59,308.22	0.0058[a]	51.99	0.0005[a]
β_{22}		1					31,936.95	0.0284[a]	2.97	0.2553
β_{33}		1					8199.60	0.2237	8.11	0.0742
Interaction										
β_{12}		1					22,268.89	0.0582	1.49	0.4124
β_{13}		1					2792.32	0.4665	8.92	0.0631
β_{23}		1					11,322.69	0.1584	5.43	0.1339
Residual	16	10	95.67		156.52		48,725.35		20.41	
Lack of fit	11	5	85.18	0.0804	142.66	0.0506	18,724.55	0.6912	14.47	0.1757
Pure error	5	5	10.49		13.86		30,000.80		5.95	
Cor total	19	19	353.80		1174.30		291,472.22		245.10	
R^2			0.7296		0.8667		0.8328		0.9167	
Adjusted R^2			0.6789		0.8417		0.6824		0.8418	
Predicted R^2			0.5361		0.7792		0.3607		0.5167	
CV (%)			13.86		12.24		13.65		9.58	
AP			12.65		19.96		6.79		13.665	

SS sum of squares, *Cor total* SS total corrected for the mean, *CV* coefficient of variation, *AP* adequate precision, *WVTR* water vapor transmission rate, *WVP* water vapor permeability

[a]p value less than 0.05 indicates model terms are significant

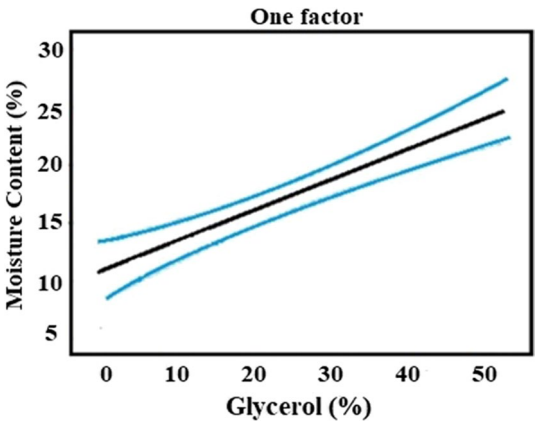

Fig. 1 One factor plot showing the significant ($p < 0.05$) linear effect of glycerol on the moisture content of film; $x_2 = 2.50\%$ and $x_3 = 7.50\%$; Blue lines show 95% confidence interval

Hydrogen bonds can be formed between the OH groups of PVOH and BCNCs and the glycerol that is easily incorporated into the PVOD/BCNCs chains. Direct interaction and chain closeness are dampened when glycerol is added to the PVOH/BCNCs/boric acid matrix. Glycerol's hydroxyl groups strongly attract water molecules, which the film network can use to its advantage by forming hydrogen bonds. It has also been shown that the increased plasticizer quantity raises the moisture content of films as per their highly hygroscopic attributes, leading to a significant force decrease among the adjoining macromolecules [10, 22, 30]. Carvalho [31], and Cazón [32] also stated that the amount of water in PVOH films rose dramatically after glycerol was added to the mixture, mainly due to the robust hydrophilic properties of glycerol, and growing the mobility of biopolymer chains due to the development free volume of molecular network. Similarly, Su [33] detected a growth in the moisture content of soy films combined with PVOH and glycerol.

Film solubility

The ability of a film to dissolve in water is a useful measure of its ability to withstand moisture when used in food packaging. Composite films' resistance to water solubility

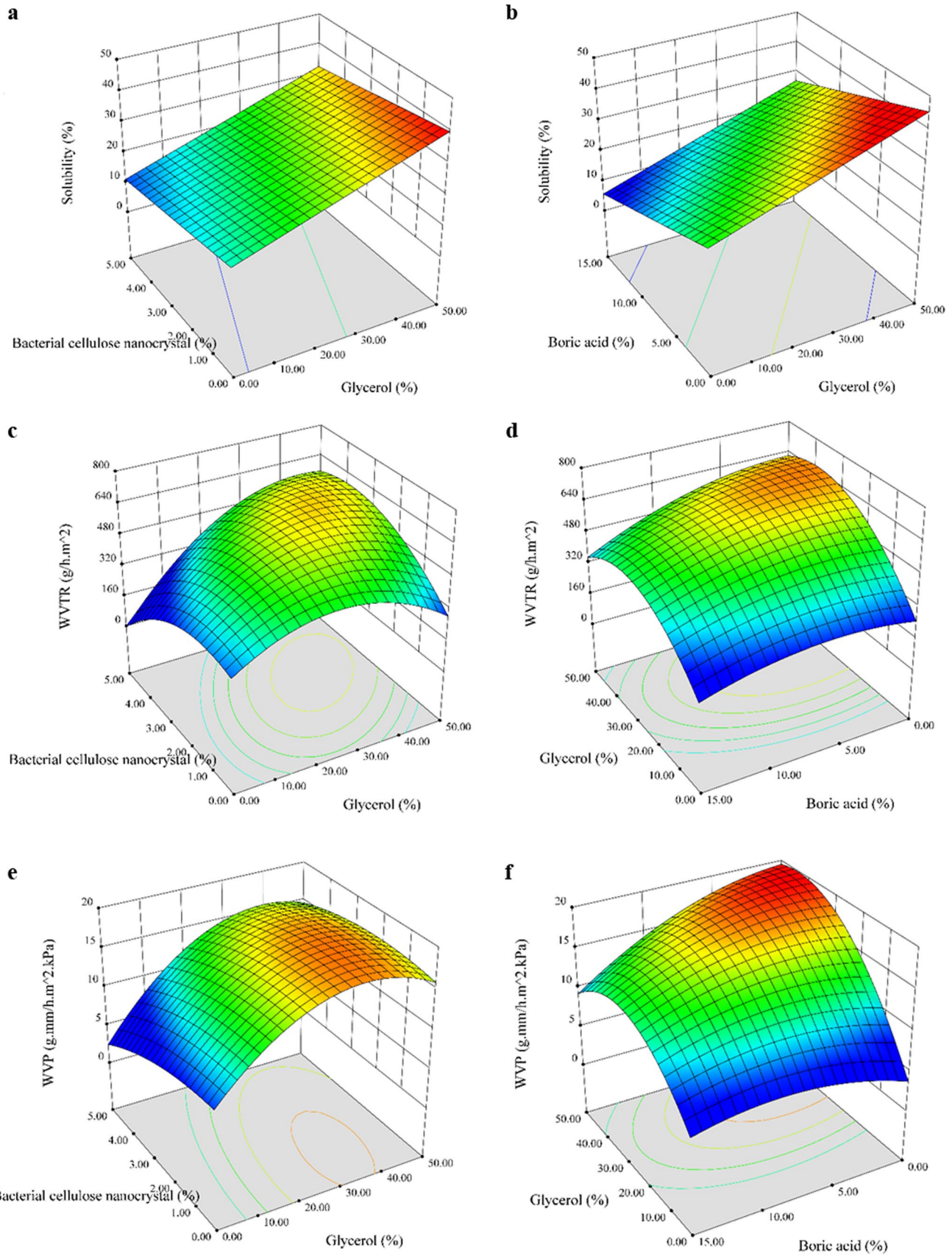
a
Solubility (%)
Bacterial cellulose nanocrystal (%)
Glycerol (%)
b
Solubility (%)
Boric acid (%)
Glycerol (%)
c
WVTR (g/h.m^2)
Bacterial cellulose nanocrystal (%)
Glycerol (%)
d
WVTR (g/h.m^2)
Glycerol (%)
Boric acid (%)
e
WVP (g.mm/h.m^2.kPa)
Bacterial cellulose nanocrystal (%)
Glycerol (%)
f
WVP (g.mm/h.m^2.kPa)
Glycerol (%)
Boric acid (%)

◂**Fig. 2** The 3D surface plots showing the significant ($p < 0.05$) interaction effects on the water solubility (**a** and **b**), WVTR (**c** and **d**), water vapor permeability (WVP) (**e** and **f**); The other independent variable in each plot is constant at coded value of 0

both maintains their structural integrity and protects the freshness of packaged foods [4, 27]. The film solubility can be affected by various parameters including the biopolymer matrix, film-forming technique, the type of plasticizer, cross-linking agent, and other reinforcement agents [16, 22]. Table 3 demonstrates that there is a statistically significant ($p < 0.02$) relationship between the linear terms of the independent factors and the water solubility of composite films. Table 3 also demonstrates that the linear increase in glycerol percentage caused the most significant effect ($p < 0.0001$) on the film solubility. The glycerol is soluble in water, so the film's water-soluble solids are expended by increasing the glycerol's amount, according to the results of other researchers [17]. The additions of boric acid decreased the film's solubility (Fig. 2a) by the formation of crosslinking linkages and reduced the mobility of materials within the film complex. In contrast, Kader [34] observed that the solubility of plasticized sorbitol PVOH film amplified with loading higher contents of boric acid.

In the case of the addition of BCNCs to PVOH film, the solubility of the prepared film was similar to neat PVOH film with no significant reduction, probably due to the contact angle of PVOH/BCNCs being lower than that of PVOH since BCNCs have functional groups like sulfur trioxide on their surface. The generation of these functional groups is attributed to the acid hydrolysis and formation of ionic bonds with water [35]. Their electrostatic repulsion interactions compensated for the excellent adhesion between PVOH and BCNCs [36, 37]. Moreover, Islam [38] stated that the water solubility of PVOH films was greatly improved with the addition of nanocellulose.

Water vapor transmission rate (WVTR)

In most food packaging cases, eliminating or minimizing the moisture transmission between food and the environment is recommended. Therefore, WVTR must be as low as possible. ANOVA and RSM plots revealed that the linear influence of boric acid and glycerol levels on WVTR was significant ($p < 0.05$). As shown in Fig. 2c, the correlation between the BCNCs/glycerol interactions and the WVTR was non-linear in the examined variable ranges. As can be observed, there was a dramatic rise in WVTR when the glycerol levels in the film matrix were raised to 35% while loading higher amounts of glycerol content kept the WVTR almost constant. With increasing the BCNCs amount in the film formulation, WVTR was slightly reduced. In addition, according to Fig. 2d, no significant differences were observed in WVTR values by increasing boric acid content in films without glycerol addition. However, the WVTR readings dropped drastically when boric acid was added to the films along with larger concentrations of glycerol. Laxmeshwar [39] and Sarwar [40] also reported that the PVOH film WVTR decreased with increasing BCNCs content, probably due to the film hydrophilicity reduction with the BCNCs percentage increase. The hydrogen bonding between BCNCs and water molecules may be responsible for this phenomenon [40].

WVP

Water vapor can be transferred from the packaging inside or outside the environment through the packaging material, impacting food safety and duration in storage [22, 41]. Based on Table 3, changes in glycerol content showed the most significant effect on WVP of films among the studied independent variables ($p < 0.0001$), followed by boric acid content ($p < 0.01$), and BCNCs content ($p < 0.03$). As evident, the quadratic model of the glycerol content was also significant ($p < 0.001$). As shown in Fig. 2e, the linear relationship between the interaction effects of boric acid, glycerol, and BCNCs contents of films on WVP values.

Moreover, an increase in glycerol from 0 to 35% raised the WVP of composite films from 8.70 to 18.15 g mm/h m^2 kPa, while the further incorporation of glycerol kept the WVP almost constant. As a hydrophilic plasticizer, glycerol possesses greater hydroxyl groups compared to PVOH and cellulose derivatives, as such, it can interact with water through hydrogen bonds. Because of this improvement in water molecule transport through the film network, WVP rates increased [12].

With increasing the BCNCs within the film matrix, WVP slightly decreased. Water diffusion through the film matrix is hindered by the presence of BCNCs because their distribution decreases the free volume of the PVOH matrix [32]. Also, according to Fig. 2f, WVP values did not significantly change by loading boric acid without the addition of glycerol. However, the simultaneous incorporation of boric acid and glycerol caused a drastic decline in the WVP of composite films. Therefore, boric acid could protect against increasing WVP in PVOH films at high glycerol concentrations. These results agreed with those of Cazón [42], who investigated the plasticizing impact of glycerol and BCNCs on PVOH. They figured out that higher concentrations of glycerol affected a significant rise in WVP of PVOH, while the incorporation of higher cellulose contents caused a slight decrease in WVP. This condition may be due to the inaccessibility of cellulose crystals to water molecules. Nevertheless, it should be noted that cellulose also contains water-resistance (hydrophobic) para-crystalline components [43]. Su [33] also observed that loading higher amounts of

glycerol raised the WVP of PVOH because of its hydrophilicity. Talja [44] reported similar results in starch-based films. Cerqueira [45] also observed a significant enhancement in WVP values of galactomannan and chitosan films by the addition of glycerol content (0.5–2%).

As indicated by the optimization results, the minimum WVP value of 0.30 g mm/h m^2 kPa in PVOH films was achieved by the regression equation and optimal values of 0.00%, 4.35%, and 1.37% for glycerol, BCNCs, and boric acid contents, respectively.

Verification of models

The optimal values of the independent variables were predicted using an optimization approach to achieve only minimum water solubility and WVP for certain reasons: 1- as the variety of responses increases, the quality of optimization results declines; 2- among moisture resistance properties of films, the moisture content is less important; 3- The WVTR is a less important response than WVP and depends on the film thickness and pressure difference between inside and outside the packaging. As per the RSM package's response optimizer tool, the following contents of variables were determined as optimal levels: 1.15% glycerol, 2.81% BCNCs, and 14.63% boric acid. The response values for moisture content, water-solubility, WVTR and WVP predicted under the suggested optimal conditions were 10.25%, 6.23%, 210.89 g/h m^2 and 6.18 g mm/h m^2 kPa, respectively. After comparing the results of six experiments to the theoretical expectations, no significant differences were found (Table 4; $p > 0.1$). As a result, the measured values agreed with the theoretical ones.

Antimicrobial activity

According to Table 5, films without boric acid (neat PVOH and boric acid blank films) did not have a surrounding inhibition zone, suggesting that boric acid was the only active antimicrobial agent in the film samples. The films with antimicrobial activity, including glycerol blank film, BCNCs blank film, and optimal film, had a weak antimicrobial effect on *Pseudomonas aeruginosa* and intense activity against *S. aureus*, *E. coli,* and *C. albicans*. Moreover, the collected results indicate that the film samples show no inhibitory effect on *B. subtilis*. Generally, the BCNCs blank film had higher antibacterial activity than the other film samples. The results indicate that by comparing the glycerol and BCNCs blank films with the optimal film, it's clear that the presence of glycerol and BCNCs in the optimal film increased and reduced antimicrobial activity against the tested microorganisms, respectively. The reason is most likely due to the greater involvement of boric acid in the presence of BCNCs

Table 4 Predicted and experimental values of the responses in optimum conditions

Independent variables	Optimum condition (g/100 g PVOH)	Response variables	Optimum condition[a]	
			Experimental[b]	Predicted[c]
Glycerol	1.15	Moisture content (%)	9.52 ± 2.43	10.25 ± 2.45
BCNCs	2.81	Water solubility (%)	5.02 ± 1.47	6.23 ± 3.13
Boric acid	14.63	WVTR (g/h m^2)	232.23 ± 8.33	210.89 ± 69.80
		WVP (g mm/h m^2 kPa)	6.94 ± 1.15	5.89 ± 1.43

WVTR water vapor transmission rate, *WVP* water vapor permeability, *BCNCs* bacterial cellulose nanocrystals, *PVOH* polyvinyl alcohol

[a]Values in each row indicates the insignificant difference between predicted and experimental values ($p > 0.1$)

[b]Mean ± standard deviation (n = 6)

[c]Mean ± standard deviation estimated on the ANOVA

Table 5 Antimicrobial activity of neat, glycerol blank, BCNCs blank, boric acid blank, and optimized PVOH films against tested microorganisms

Microorganisms	Inhibition zone (mm^2)*				
	Neat PVOH	Glycerol blank	BCNCs blank	Boric acid blank	Optimum film
Escherichia coli	0.00	42.81^{ac}	103.40^{Ba}	0.00	79.60^{Bb}
Staphylococcus aureus	0.00	48.94^{Ac}	92.80^{Ba}	0.00	65.87^{Bb}
Pseudomonas aeruginosa	0.00	9.71^{Cb}	33.62^{Ca}	0.00	28.61^{Ca}
Bacillus subtilis	0.00	0.00	0.00	0.00	0.00
Candida albicans	0.00	24.43^{Bc}	154.62^{Aa}	0.00	104.59^{Ab}

*Mean ± standard deviation (n = 3). Different small and capital letters represent significant differences ($p < 0.05$) in each row and column

or its availability in the presence of glycerol. Boric acid dissolves in moisture by increasing the access to an agar medium and can diffuse to a certain radius of the film disc and show its antimicrobial effects. Cellulose nanocrystals do not possess inherent antibacterial properties, hence imposing constraints on their applicability in functional packaging. Moreover, the majority of research attempts have concentrated on investigating the mechanical properties of cellulose nanocrystals inside polymer matrices. However, there is a lack of studies exploring the enhancement of the functional characteristics of cellulose nanocrystals prior to the creation of composites with PVA/BCNCs. Cellulose nanocrystals possess a considerable number of hydroxyl groups on their surface, facilitating convenient modification. Various methods for surface modification, including esterification, oxidation, and salinization, have been documented in the literature. Therefore, the synthesis of multifunctional nanomaterials can be readily achieved through chemical grafting [16].

According to Table 5, *B. subtilis* (Gram-positive) and *C. albicans* were the most and minor resistant strains to the optimal film samples. Bursali [46] reported that starch/PVOH composite film crosslinked with boric acid had no antimicrobial activity against *B. subtilis*. They also stated that starch/PVOH crosslinked film containing glutaraldehyde and boric acid showed a more excellent inhibition zone against *S. aureus* (13 mm), *E. coli* (14 mm), and *C. albicans* (14 mm) compared to *Pseudomonas aeruginosa* (12 mm). In contrast, Sarwar [40] detected that the existence of BCNCs in PVOH improved their antimicrobial activity. They found that BCNCs not only suppressed *E.coli* pathogenic strain (14.00 ± 0.70 mm) (gram-negative) but also showed an excellent protective effect against gram-positive bacteria (13.60 ± 0.68 mm). Tripathi [47] stated that chitosan/PVOH films with glutaraldehyde as a crosslinker had more antimicrobial activity against *E. coli* (1.5 mm) and *B. subtilis* (1.4 mm) in comparison to *S. aureus* (1.2 mm).

Soil burial degradation test

Taking into account the environmental hazards of synthetic polymers, degradability plays a vital role in food packaging applications. Burial in soil provides a naturalistic setting where variables like humidity, temperature, soil type, and microbial population fluctuate seasonally and are less strictly controlled [28, 48]. As shown in Fig. 3, the biodegradability changes of neat, optimal, and blank PVOH films during 6 months of storage. The glycerol blank film presented much lower biodegradability (approximately 20 wt%) than neat (about 24 wt%) and optimal (around 31 wt%) PVOH films at the end of six months. As the time progressed, the tested samples was quickly biodegraded and numerous large cavities, small

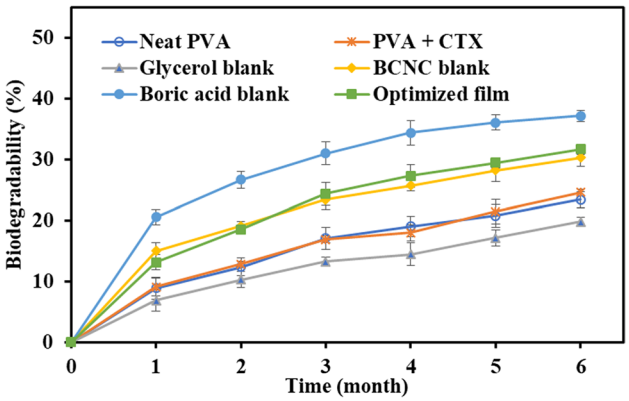

Fig. 3 Degradability of neat, glycerol blank, BCNCs blank, boric acid blank, and optimized PVOH films

holes, and cracks are made on the surface of the films leading to channels formations and promote the entry of water and microorganisms, thus producing the biodegradation process of the polymer matrixes.

Despite having moisture-resistant compounds, including BCNCs and boric acid, and antimicrobial agent (boric acid), the higher biodegradability of the optimal film with respect to neat PVOH film (as control) may be associated with increased sensitivity of films to moisture, due to the glycerol addition, as well as to the degradability of glycerol itself by microorganisms. The trend of the biodegradability changes in optimal and blank BCNCs films shows no significant difference between them (Fig. 3). Since the nanocellulose is an organic compound, it was expected that its addition to the optimal film would increase its biodegradability compared to BCNCs blank. However, it is conceivable that the specific property of BCNCs in increasing the optimal film resistance to water decreased microbial activities. Hence, the contrast between these two traits in BCNCs did not change the biodegradability of the optimal film.

According to Fig. 3, the boric acid blank film showed much higher biodegradability than the optimal film (about 37% after six months), suggesting that the boric acid decreased the biodegradability. Similarly, Kader [34] reported that the boric acid as a crosslinker caused slow degradation in pregelatinized maize starch/PVOH/boric acid composite, which could be ascribed to the chemical interaction through hydrogen bonding between pregelatinized maize starch and PVOH incorporated with the boric acid. Moreover, Islam [38] detected that the degradation rate of the PVOH film with nanocellulose increased compared to neat PVOH because the nanocellulose is more biodegradable than PVOH. Ibrahim [49] also reported the PVOH matrix degradation was faster in the presence of the nanospherical cellulose particles.

XRD

Crystallinity is associated with the arrangement of molecules in the films and is related to the stability of the material [22]. Indeed, the melting point of the molecule increases with a higher amount of crystalline structure. The XRD patterns of neat, optimal PVOH films and blanks are shown in Fig. 4. A strong peak at 2θ = 23°, characteristic of neat PVOH, referring to the (101) crystal plane, was detected, suggesting the semi-crystalline nature of PVOH [8]. The addition of various constituents can result in irregularities in the structure of films, and, thus, in a crystallinity decrease. As evident in the diffraction patterns of the other films (Fig. 4), the height of the characteristic crystalline peak of neat PVOH film was reduced by adding other constituents, resulting in a decrease in the film stability. However, there are no shifts in crosslinked films. Chen [13] also reported that PVOH film (whether crosslinked or not) presents only one characteristic peak at 2θ = 19.8°. They also observed that in PVOH crosslinked film with boric acid, the characteristic peak does not make any shifts. However, in the crosslinked film, the relative intensity of the characteristic peak decreases due to the reduction of the crystallinity and interactions between the polymer chains and the boric acid. In the case of glycerol, Su [33] reported that the XRD patterns are less intense when higher contents of glycerol are introduced in the film matrix, signifying that the presence of glycerol decreases the crystallinity of composite films. It is believed that glycerol can penetrate the crystalline structure, regulate soy protein isolate/PVOH microstructure, and increase the toughness by decreasing the crystallinity degree. Lu [50] also reported similar results and stated that glycerol penetrates the macromolecular blend and destroys the crystallinity of the blend. In the XRD pattern of the BCNCs blank film, only the characteristic diffraction peak of PVOH appeared. However, in glycerol blank, boric acid blank, and optimized films, three peaks (2θ values of 17°, 20°, and 27°) were identified around the PVOH crystalline peak, which is similar to those of the BCNCs [51]. Sarwar [40] observed that the peak at 2θ = 19.8° corresponds to the hydrated crystalline structure of neat PVOH. At the same time, the weak diffraction of nanocellulose was observed at around 2θ = 16.2°, indicating the amorphous structure, which is very low in intensity. Meanwhile, other researchers reported other diffraction peaks located at 2θ = 22.4° and 2θ = 34.4°, characteristic of the nanocellulose [52]. Similarly, Ching [53] reported that the crystallinity of PVOH film containing 3 wt% nanocellulose was lower than that observed in neat PVOH. The original crystallinity of PVOH film was never attained in the nanocellulose-reinforced PVOH composite because of the heterogonous phase nucleation in the synthesizing solution [54]. On the contrary, Jancy [55] stated that in the XRD pattern of cellulose nanoparticles-PVOH bionanocomposite film, the 23.05° diffraction peak of the bionanocomposite film postulates that the advanced precision of the crystal matrix of cellulose nanoparticles has improved the crystallinity degree. Due to the incorporation of cellulose nanoparticles, the major diffraction peaks were observed at 22.2°, 31°, and 34.8°. The average molecular distance of the layers inside the crystals in Table 6 shows a slight difference among different treatments. Therefore, the amount of crystal compression was the same in different film samples.

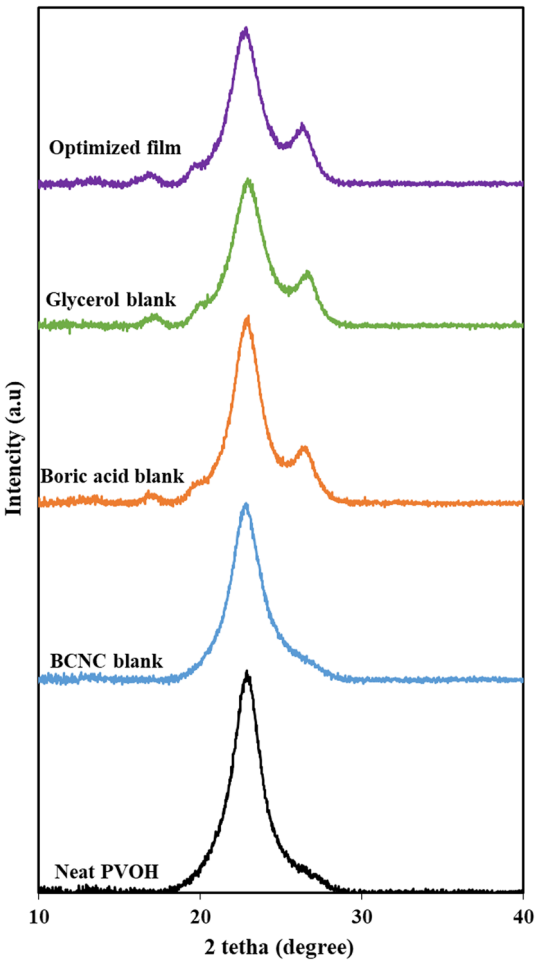

Fig. 4 XRD patterns of neat, glycerol blank, BCNCs blank, boric acid blank, and optimized PVOH films

Thermal properties

The heat stability of the film indicates its tolerance to temperature changes. The type of polymers, the method used for polymers' crosslinking, and the kind of crosslinking agents and plasticizers and their concentration are the main factors able to influence the thermal stability of crosslinked films. The DSC analysis was performed to investigate the thermal stability of the PVOH films, as indicated in Fig. 5, and the results are presented in Table 6.

Table 6 DSC indices of neat, glycerol blank, BCNCs blank, boric acid blank, and optimized PVOH films

DSC indices	Unit	Treatments				
		Neat PVOH	Glycerol blank	BCNCs blank	Boric acid blank	Optimum
T_g	°C	78	99	71	69	91
T_m	°C	223	196	193	221	196
ΔH_m	J/g	67	41	40	52	40
T_c	°C	189	152	114	190	150
ΔH_c	J/g	62	24	25	51	18
X_c	%	43	25	23	29	22

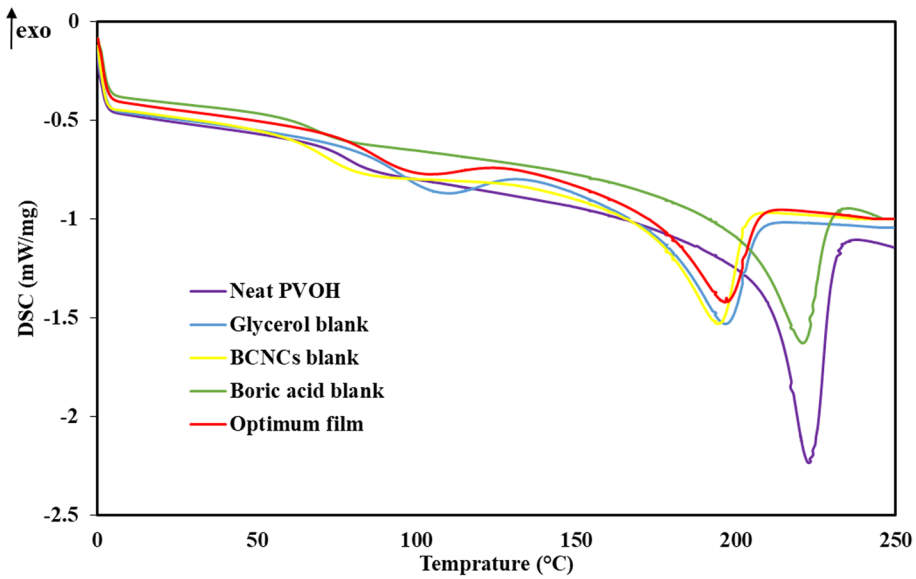

Fig. 5 DSC curves of neat, glycerol blank, BCNCs blank, boric acid blank, and optimized PVOH films

Table 6 demonstrates the DSC indices of prepared films. The glass transition temperature (T_g) value of a film is a valuable technique to study the amorphous area changes. Results showed that the optimized film had a greater T_g value (91 °C) than neat PVOH film (78 °C), BCNCs (71 °C), and boric acid (69 °C) blank films. Therefore, it can be concluded that the addition of BCNCs and boric acid increased the thermal stability of the film, due to the hydrogen bonds between BCNCs, boric acid, and −OH groups of PVOH [11]. Moreover, boric acid crosslinks the intermolecular and intramolecular chains in amorphous areas related to chemical reactions between PVOH chains and boric acid. Therefore, the molecular motions of PVOH polymer chains are restricted [56]. Chen [11] also, reported that the boric acid-induced PVOH film had higher thermal stability than the neat PVOH film. Furthermore, Cazón [42] showed that the microcrystalline cellulose increased the thermal stability of the PVOH films, due to the increased interaction between the constituents. The T_g value of glycerol blank film (99 °C) was higher than that of the optimized film, indicating that the addition of glycerol reduced the thermal stability, due to the consequent lower crystallinity of PVOH films in the presence of glycerol compared to blank glycerol film. This effect was also observed in plasticized PVOH-soy protein isolate film with glycerol [33]. In contrast, Cazón [42] reported that glycerol improved the thermal stability of PVOH films due to the increased hydrogen bonding between glycerol and PVOH.

The DSC curves of the composite films as a function of temperature are shown in Fig. 5. The DSC curves of the prepared PVOH films (Fig. 5) can be separated into two areas. The first area (30–100 °C) relates to the volatilization of water from the PVOH films, and the second area (170–240 °C) relates to the components' depolymerization of the developed films [57]. The onset of the melting temperature (T_o) and the melting point (T_m) of the neat PVOH film reduced after incorporating with other constituents in the film matrix: T_o and T_m for neat PVOH film were 209 and 222 °C, respectively, higher than those for boric acid blank (199, and 221 °C), glycerol blank (172, and 196 °C), BCNCs blank (171, and 193 °C), and optimal (171, and 196 °C) films. After adding the boric acid, the DSC curve peak shifts to the left. The T_m of the boric acid blank film is almost equal to the neat PVOH film. However, the neat

PVOH film melting peak was larger and sharper than that of the boric acid blank film. Besides, the fusion enthalpy of PVOH (ΔH_m) was reduced from 67 to about 40 J/g using boric acid in the film-forming matrix. These shifts in DSC curves and reduction in T_o, T_m, and ΔH_m values may be owing to the reduced domain size and amount of the crystallinity of the prepared PVOH films compared to neat PVOH film, which is associated with slowing down the molecular mobility by crosslinking [8, 56]. The crosslinking between boric acid and the linear PVOH chains and the B−O−C bonds inhibit a crystalline formation while growing the quasicrystalline structure and lowering the free volume in the amorphous areas of PVOH [58]. These results are also proved by the lower crystallinity of films as scrutinized by XRD analysis (Fig. 4). Similarly, Woo [58] observed that neat PVOH film presented a sharp melting peak at 220 °C. However, the crosslinked films showed a broad peak at the lower temperature (80–180 °C). Furthermore, a new peak appeared at a lower temperature zone (80–120 °C) for the boric acid-containing films (BCNCs blank, glycerol blank, and optimized films), which may be related to the quasicrystalline phase melting [56].

Conclusions

The addition of functional components was prompted by the weaknesses observed in some aspects of biodegradable films. In this study, the effects of various functional substances, including BCNCs, boric acid, and glycerol on the physical, mechanical, antimicrobial, and thermal properties of the PVA films were evaluated. The optimal moisture content, water-solubility, WVTR, and WVP were respectively predicted at 10.25%, 6.23%, 210.89 g/h m^2, and 6.18 g mm/h m^2 kPa. Boric acid was the only active antimicrobial compound in the film samples. Along with boric acid in the optimized film, the presence of glycerol and BCNCs increased and decreased the antimicrobial activity, respectively. Nanocrystals did not affect the biodegradability of films. However, glycerol and boric acid showed remarkable positive and negative effects on biodegradability, respectively. Based on the XRD results, the crystallinity of neat PVOH decreased due to the addition of various constituents. The thermogram of the optimized film sample showed a higher T_g than neat PVOH film, suggesting an increase in thermal stability. The optimal PVOH film exhibited antibacterial properties, demonstrated increased resistance to moisture, and was thermally stable. These are all desirable qualities for usage in the packaging and coating of food and pharmaceuticals. Therefore, it is anticipated that the PVA-based nanocomposite functional film will serve as an active film, hence enhancing the shelf life of packaged food products. There has been a notable increase in the prevalence of food-borne diseases that are prompting significant attention and worry within the realm of public health. In addressing this issue, the implementation of antibacterial packaging has emerged as a potentially crucial strategy for ensuring the safety and security of food.

Data Availability The data that has been used is confidential.

References

1. S.R. Yousefi, H.A. Alshamsi, O. Amiri, M. Salavati-Niasari, Synthesis, characterization and application of Co/Co_3O_4 nanocomposites as an effective photocatalyst for discoloration of organic dye contaminants in wastewater and antibacterial properties. J. Mol. Liq. **337**, 116405 (2021)
2. S.R. Yousefi, O. Amiri, M. Salavati-Niasari, Control sonochemical parameter to prepare pure $Zn_{0.35}Fe_{2.65}O_4$ nanostructures and study their photocatalytic activity. Ultrason. Sonochem. **58**, 104619 (2019)
3. W. Wang, Z. Yu, F.K. Alsammarraie, F. Kong, M. Lin, A. Mustapha, Properties and antimicrobial activity of polyvinyl alcohol-modified bacterial nanocellulose packaging films incorporated with silver nanoparticles. Food Hydrocoll. **100**, 105411 (2020)
4. R. Abedi-Firoozjah, E. Parandi, M. Heydari, A. Kolahdouz-Nasiri, M. Bahraminejad, R. Mohammadi, M. Rouhi, F. Garavand, Betalains as promising natural colorants in smart/active food packaging. Food Chem. **424**, 136408 (2023)
5. M. Heydari, K. Carbone, F. Gervasi, E. Parandi, M. Rouhi, O. Rostami, R. Abedi-Firoozjah, A. Kolahdouz-Nasiri, F. Garavand, R. Mohammadi, Cold plasma-assisted extraction of phytochemicals: a review. Foods **12**(17), 3181 (2023)
6. R. Zibaei, S. Hasanvand, Z. Hashami, Z. Roshandel, M. Rouhi, J. de Toledo Guimarães, A.M. Mortazavian, Z. Sarlak, R. Mohammadi, Applications of emerging botanical hydrocolloids for edible films: a review. Carbohydr. Polym. **256**, 117554 (2021)
7. M.A. Moghadam, R. Mohammadi, E. Sadeghi, M.A. Mohammadifar, M. Nejatian, M. Fallah, M. Rouhi, Preparation and characterization of poly (vinyl alcohol)/gum tragacanth/cellulose nanocomposite film. J. Appl. Polym. Sci. **138**(28), 50672 (2021)
8. H. Abral, A. Atmajaya, M. Mahardika, F. Hafizulhaq, D. Handayani, S. Sapuan, R. Ilyas, Effect of ultrasonication duration of polyvinyl alcohol (PVA) gel on characterizations of PVA film. J. Market. Res. **9**(2), 2477–2486 (2020)
9. M. Taghizadeh, S. Aryan, M. Rouhi, M.R. Sobhiyeh, F. Askari, M. Gholipourmalekabadi, S. Sohrabvandi, M.Z. Khajavi, S.M. Davachi, A. Abbaspourrad, Photo-crosslinked gelatin–polyvinyl alcohol composite films: UV–riboflavin treatment for improving functional properties. J. Food Process. Preserv. **44**(7), e14550 (2020)
10. F. Garavand, M. Rouhi, S.H. Razavi, I. Cacciotti, R. Mohammadi, Improving the integrity of natural biopolymer films used in food packaging by crosslinking approach: a review. Int. J. Biol. Macromol. **104**, 687–707 (2017)
11. C. Chen, Y. Chen, J. Xie, Z. Xu, Z. Tang, F. Yang, K. Fu, Effects of montmorillonite on the properties of cross-linked poly (vinyl alcohol)/boric acid films. Prog. Org. Coat. **112**, 66–74 (2017)
12. M. Rouhi, S.H. Razavi, S.M. Mousavi, Optimization of crosslinked poly (vinyl alcohol) nanocomposite films for mechanical properties. Mater. Sci. Eng. C **71**, 1052–1063 (2017)

13. J. Chen, Y. Li, Y. Zhang, Y. Zhu, Preparation and characterization of graphene oxide reinforced PVA film with boric acid as crosslinker. J. Appl. Polym. Sci. **132**(22), 1–8 (2015)
14. K. Park, Y. Oh, P.K. Panda, J. Seo, Effects of an acidic catalyst on the barrier and water resistance properties of crosslinked poly (vinyl alcohol) and boric acid films. Prog. Org. Coat. **173**, 107186 (2022)
15. X. Li, P. Bandyopadhyay, M. Guo, N.H. Kim, J.H. Lee, Enhanced gas barrier and anticorrosion performance of boric acid induced cross-linked poly(vinyl alcohol-co-ethylene)/graphene oxide film. Carbon **133**, 150–161 (2018)
16. L. Meng, J. Li, X. Fan, Y. Wang, Z. Xiao, H. Wang, D. Liang, Y. Xie, Improved mechanical and antibacterial properties of polyvinyl alcohol composite films using quaternized cellulose nanocrystals as nanofillers. Compos. Sci. Technol. **232**, 109885 (2023)
17. M. Babaee, F. Garavand, A. Rehman, S. Jafarazadeh, E. Amini, I. Cacciotti, Biodegradability, physical, mechanical and antimicrobial attributes of starch nanocomposites containing chitosan nanoparticles. Int. J. Biol. Macromol. **195**, 49–58 (2022)
18. H.C. Oyeoka, C.M. Ewulonu, I.C. Nwuzor, C.M. Obele, J.T. Nwabanne, Packaging and degradability properties of polyvinyl alcohol/gelatin nanocomposite films filled water hyacinth cellulose nanocrystals. J. Bioresour. Bioprod. **6**(2), 168–185 (2021)
19. L. Wang, C. Chen, J. Wang, D.J. Gardner, M. Tajvidi, Cellulose nanofibrils versus cellulose nanocrystals: comparison of performance in flexible multilayer films for packaging applications. Food Packag. Shelf Life **23**, 100464 (2020)
20. M. Shirani, E. Parandi, H.R. Nodeh, B. Akbari-Adergani, F. Shahdadi, Development of a rapid efficient solid-phase microextraction: an overhead rotating flat surface sorbent based 3-D graphene oxide/lanthanum nanoparticles@ Ni foam for separation and determination of sulfonamides in animal-based food products. Food Chem. **373**, 131421 (2022)
21. H. Sereshti, S. Soltani, N. Sridewi, E. Salehi, E. Parandi, H. Rashid Nodeh, S. Shahabuddin, Solid phase extraction penicillin and tetracycline in human serum using magnetic graphene oxide-based sulfide nanocomposite. Magnetochemistry **9**(5), 132 (2023)
22. F. Garavand, S. Jafarzadeh, I. Cacciotti, N. Vahedikia, Z. Sarlak, Ö. Tarhan, S. Yousefi, M. Rouhi, R. Castro-Muñoz, S.M. Jafari, Different strategies to reinforce the milk protein-based packaging composites. Trends Food Sci. Technol. **123**, 1–14 (2022)
23. E. Parandi, M. Mousavi, E. Assadpour, H. Kiani, S.M. Jafari, Sesame protein hydrolysate-gum Arabic Maillard conjugates for loading natural anthocyanins: characterization, in vitro gastrointestinal digestion and storage stability. Food Hydrocoll. **148**, 109490 (2024)
24. F. Amiratashani, M.S. Yarmand, H. Kiani, G. Askari, K.K. Naeini, E. Parandi, Comprehensive structural and functional characterization of a new protein-polysaccharide conjugate between grass pea protein (*Lathyrus sativus*) and xanthan gum produced by wet heating. Int. J. Biol. Macromol. **254**, 127283 (2024)
25. B. Hadi Jume, E. Parandi, M. Nouri, B. Aghel, A. Gouran, H. Rashidi Nodeh, H. Kamyab, J. Cho, S. Rezania, Optimization of microreactor-assisted transesterification for biodiesel production using bimetal zirconium-titanium oxide doped magnetic graphene oxide heterogeneous nanocatalyst. Chem. Eng. Process. Process Intensif. **191**, 109479 (2023)
26. M. Safaripour, E. Parandi, B. Aghel, A. Gouran, M. Saidi, H.R. Nodeh, Optimization of the microreactor-intensified transesterification process using silver titanium oxide nanoparticles decorated magnetic graphene oxide nanocatalyst. Process Saf. Environ. Prot. **173**, 495–506 (2023)
27. S. Pourjavaher, H. Almasi, S. Meshkini, S. Pirsa, E. Parandi, Development of a colorimetric pH indicator based on bacterial cellulose nanofibers and red cabbage (*Brassica oleraceae*) extract. Carbohydr. Polym. **156**, 193–201 (2017)
28. I. Thakore, S. Desai, B. Sarawade, S. Devi, Studies on biodegradability, morphology and thermo-mechanical properties of LDPE/modified starch blends. Eur. Polym. J. **37**(1), 151–160 (2001)
29. B.H. Jume, N. Valizadeh Dana, M. Rastin, E. Parandi, N. Darajeh, S. Rezania, Sulfur-doped binary layered metal oxides incorporated on pomegranate peel-derived activated carbon for removal of heavy metal ions. Molecules **27**(24), 8841 (2022)
30. M. Shirani, A. Aslani, F. Ansari, E. Parandi, H.R. Nodeh, E. Jahanmard, Zirconium oxide/titanium oxide nanorod decorated nickel foam as an efficient sorbent in syringe filter based solid-phase extraction of pesticides in some vegetables. Microchem. J. **189**, 108507 (2023)
31. R. Carvalho, T. Maria, I. Moraes, P. Bergo, E. Kamimura, A. Habitante, P. Sobral, Study of some physical properties of biodegradable films based on blends of gelatin and poly (vinyl alcohol) using a response-surface methodology. Mater. Sci. Eng. C **29**(2), 485–491 (2009)
32. P. Cazón, G. Velazquez, M. Vázquez, Characterization of mechanical and barrier properties of bacterial cellulose, glycerol and polyvinyl alcohol (PVOH) composite films with eco-friendly UV-protective properties. Food Hydrocoll. **99**, 105323 (2020)
33. J.-F. Su, Z. Huang, K. Liu, L.-L. Fu, H.-R. Liu, Mechanical properties, biodegradation and water vapor permeability of blend films of soy protein isolate and poly (vinyl alcohol) compatibilized by glycerol. Polym. Bull. **58**(5), 913–921 (2007)
34. M.A. Kader, M.A. Khan, M.E. Molla, Effect of boric acid on the properties of sorbitol plasticized starch/PVA blends. Eng. Int. **5**(2), 63–74 (2017)
35. M. Asad, N. Saba, A.M. Asiri, M. Jawaid, E. Indarti, W. Wanrosli, Preparation and characterization of nanocomposite films from oil palm pulp nanocellulose/poly (vinyl alcohol) by casting method. Carbohydr. Polym. **191**, 103–111 (2018)
36. Z.W. Abdullah, Y. Dong, I.J. Davies, S. Barbhuiya, PVA, PVA blends, and their nanocomposites for biodegradable packaging application. Polym. Plastics Technol. Eng. **56**(12), 1307–1344 (2017)
37. M. Shirani, A. Aslani, S. Sepahi, E. Parandi, A. Motamedi, E. Jahanmard, H.R. Nodeh, B. Akbari-Adergani, An efficient 3D adsorbent foam based on graphene oxide/AgO nanoparticles for rapid vortex-assisted floating solid phase extraction of bisphenol A in canned food products. Anal. Methods **14**(26), 2623–2630 (2022)
38. N. Islam, S. Proma, A. Rahman, A. Chakraborty, Preparation and biodegradation of nanocellulose reinforced polyvinyl alcohol blend films in bioenvironmental media. Chem. Sci. Int. J. **19**, 1–8 (2017)
39. S.S. Laxmeshwar, D. Madhu Kumar, S. Viveka, G. Nagaraja, Preparation and properties of biodegradable film composites using modified cellulose fibre-reinforced with PVA. Int. Scholarly Res. Not. **2012**, 154314 (2012)
40. M.S. Sarwar, M.B.K. Niazi, Z. Jahan, T. Ahmad, A. Hussain, Preparation and characterization of PVA/nanocellulose/Ag nanocomposite films for antimicrobial food packaging. Carbohydr. Polym. **184**, 453–464 (2018)
41. E. Parandi, M. Pero, H. Kiani, Phase change and crystallization behavior of water in biological systems and innovative freezing processes and methods for evaluating crystallization. Discover Food **2**(1), 6 (2022)
42. P. Cazón, G. Velazquez, M. Vázquez, Novel composite films from regenerated cellulose-glycerol-polyvinyl alcohol: mechanical and barrier properties. Food Hydrocoll. **89**, 481–491 (2019)
43. A.H. Bedane, M. Eić, M. Farmahini-Farahani, H. Xiao, Water vapor transport properties of regenerated cellulose and nanofibrillated cellulose films. J. Membr. Sci. **493**, 46–57 (2015)
44. R.A. Talja, H. Helén, Y.H. Roos, K. Jouppila, Effect of various polyols and polyol contents on physical and mechanical properties

of potato starch-based films. Carbohydr. Polym. **67**(3), 288–295 (2007)
45. M.A. Cerqueira, B.W. Souza, J.A. Teixeira, A.A. Vicente, Effect of glycerol and corn oil on physicochemical properties of polysaccharide films—a comparative study. Food Hydrocoll. **27**(1), 175–184 (2012)
46. E.A. Bursali, S. Coskun, M. Kizil, M. Yurdakoc, Synthesis, characterization and in vitro antimicrobial activities of boron/starch/polyvinyl alcohol hydrogels. Carbohydr. Polym. **83**(3), 1377–1383 (2011)
47. S. Tripathi, G. Mehrotra, P. Dutta, Physicochemical and bioactivity of cross-linked chitosan–PVA film for food packaging applications. Int. J. Biol. Macromol. **45**(4), 372–376 (2009)
48. M. Esmaeili Bidhendi, E. Parandi, M. Mahmoudi Meymand, H. Sereshti, H. Rashidi Nodeh, S.-W. Joo, Y. Vasseghian, N. Mahmoudi Khatir, S. Rezania, Removal of lead ions from wastewater using magnesium sulfide nanoparticles caged alginate microbeads. Environ. Res. **216**, 114416 (2023)
49. M.M. Ibrahim, W.K. El-Zawawy, M.A. Nassar, Synthesis and characterization of polyvinyl alcohol/nanospherical cellulose particle films. Carbohydr. Polym. **79**(3), 694–699 (2010)
50. Y. Lu, L. Weng, L. Zhang, Morphology and properties of soy protein isolate thermoplastics reinforced with chitin whiskers. Biomacromolecules **5**(3), 1046–1051 (2004)
51. H. Yousefi, M. Faezipour, S. Hedjazi, M.M. Mousavi, Y. Azusa, A.H. Heidari, Comparative study of paper and nanopaper properties prepared from bacterial cellulose nanofibers and fibers/ground cellulose nanofibers of canola straw. Ind. Crops Prod. **43**, 732–737 (2013)
52. W. Zhang, X. He, C. Li, X. Zhang, C. Lu, X. Zhang, Y. Deng, High performance poly (vinyl alcohol)/cellulose nanocrystals nanocomposites manufactured by injection molding. Cellulose **21**(1), 485–494 (2014)
53. Y.C. Ching, A. Rahman, K.Y. Ching, N.L. Sukiman, H.C. Cheng, Preparation and characterization of polyvinyl alcohol-based composite reinforced with nanocellulose and nanosilica. BioResources **10**(2), 3364–3377 (2015)
54. A. Mandal, D. Chakrabarty, Studies on the mechanical, thermal, morphological and barrier properties of nanocomposites based on poly (vinyl alcohol) and nanocellulose from sugarcane bagasse. J. Ind. Eng. Chem. **20**(2), 462–473 (2014)
55. S. Jancy, R. Shruthy, R. Preetha, Fabrication of packaging film reinforced with cellulose nanoparticles synthesised from jack fruit non-edible part using response surface methodology. Int. J. Biol. Macromol. **142**, 63–72 (2020)
56. M. Lim, H. Kwon, D. Kim, J. Seo, H. Han, S.B. Khan, Highly-enhanced water resistant and oxygen barrier properties of cross-linked poly (vinyl alcohol) hybrid films for packaging applications. Prog. Org. Coat. **85**, 68–75 (2015)
57. P. Cazón, M. Vázquez, G. Velazquez, Cellulose–glycerol–polyvinyl alcohol composite films for food packaging: evaluation of water adsorption, mechanical properties, light-barrier properties and transparency. Carbohydr. Polym. **195**, 432–443 (2018)
58. J.Y. Woo, E.J. Shin, Y.H. Lee, Effect of boric acid treatment on the crystallinity and drawability of poly (vinyl alcohol)–iodine complex films. Polym. Bull. **65**(2), 169–180 (2010)